

Cone penetration testing to constrain the calibration process of a sand plasticity model for nonlinear deformation analysis

A. Chiaradonna

University of L'Aquila, L'Aquila, Italy

T.J. Carey

The University of British Columbia, Vancouver, Canada

K. Ziotopoulou & J.T. DeJong

University of California at Davis, Davis, USA

ABSTRACT: A reliable prediction of liquefaction-induced damage typically requires nonlinear deformation analyses with an advanced constitutive soil model calibrated to the site conditions. The calibration of constitutive models can be performed by relying primarily on a combination of commonly available properties and empirical or semi-empirical relationships, on laboratory tests on site-specific soils, on in-situ penetration tests, or a combination thereof. Chiaradonna et al. (2022) described a laboratory-based calibration approach of the PM4Sand constitutive model and evaluated the prediction accuracy against the response of a centrifuge experiment of a submerged slope. This paper addresses an alternate calibration approach in which the PM4Sand model is calibrated using centrifuge in-situ CPT data. The model performance for the resulting calibration is evaluated against the centrifuge experimental data and prior simulations from Chiaradonna et al. (2022). In this case, the CPT-based calibration resulted in more accurate estimations of the dynamic response and permanent displacements.

1 INTRODUCTION

A reliable prediction of liquefaction-induced damage usually requires performing nonlinear deformation analyses by adopting advanced constitutive soil models. Constitutive model calibration protocols have been developed to guide the selection of parameters, firstly driven by the goal to reproduce the soil element behavior as observed in laboratory element tests and, if tests are not available, against the broader body of data and engineering relationships in the literature. For larger scale experiments, the use of in-flight miniature Cone Penetration Tests (CPT) in centrifuge testing has provided system level soil properties and better definition of soil conditions before and after any applied shaking (Kim et al. 2016; Khosravi et al. 2018; Moug et al. 2019; Darby et al. 2019; Carey et al. 2020). Darby et al. (2019) used CPT soundings collected prior to multiple shaking events to define liquefaction triggering correlations in a centrifuge experiment. The cyclic resistance for the investigated sand in the experiment was lower than that inferred from case history-based liquefaction triggering correlations. Data from in-flight miniaturized CPTs strongly constrain several soil parameters, e.g., relative density D_R , and were therefore useful to define model calibration parameters.

Chiaradonna et al. (2022) modelled the dynamic response of a centrifuge experiment consisting of a submerged 10-degree slope of a poorly graded clean sand at a D_R of 63% (Carey et al. 2022a). Shaking was imposed by applying a 1 Hz at the base of the model container. CPTs were pushed using a 10 mm cone in the experiment prior to and following shaking, but were not considered in the calibration performed by Chiaradonna et al. (2022).

The critical state compatible, stress ratio-based, bounding surface plasticity constitutive model PM4Sand (Boulanger & Ziotopoulou 2017), implemented in the commercial finite-difference platform FLAC (Itasca, 2016) was adopted in the simulations. The primary input parameters of the model are the apparent relative density (D_R), the shear modulus coefficient (G_0), and the contraction rate parameter (h_{po}). A laboratory-based calibration was defined on the results of undrained cyclic direct simple shear tests performed on reconstituted samples (Humire et al. 2022). The simulation of the centrifuge test by adopting the laboratory-based calibration reasonably simulated the pore pressure and acceleration time histories, while the permanent horizontal displacements were overpredicted by a factor of three (Chiaradonna et al. 2022).

In this paper, the aforementioned simulation was revisited by calibrating PM4Sand parameters using the cone tip resistance as measured in the centrifuge by Carey et al. 2022a. The D_R is the target value of 63%, which was verified through a pre-shaking cone penetration test (Carey et al. 2022a). The soil behavior at small strains (i.e., G_0) was estimated by the measured cone tip resistance through the application of several literature relationships, whose efficacy was verified against the shear moduli based on the measured shear wave velocity. The cyclic resistance ratio (CRR), which is primarily controlled by the contraction rate parameter (h_{po}) in PM4Sand, was estimated through the normalized cone tip resistance measured in the experiment and the CPT-based empirical triggering liquefaction chart by Boulanger & Idriss (2014).

The comparison between simulated and experimental soil response is made to verify that in-flight CPT testing in the centrifuge experiments properly measures the cyclic strength of soils. In addition, the comparison between the CPT-based calibration and the calibration based on cyclic laboratory tests performed by Chiaradonna et al. (2022) is also discussed.

2 EXPERIMENTAL PROGRAM

2.1 Overview of centrifuge test

A 14 m-high submerged embankment with a 10-degree slope constructed with a uniform profile of sand was tested in a rigid container at 40g using the 9-m radius centrifuge at the Center for Geotechnical

Modeling located at the University of California, Davis (Figure 1). The soil was a clean poorly graded sand, hereafter called 100A sand (Sturm 2019). The physical properties of the 100A sand are $e_{min} = 0.579$, $e_{max} = 0.881$, $D_{50} = 0.18\text{mm}$, $C_u = 1.68$, and $G_s = 2.62$. The embankment was dry-pluviated to a target $D_R = 63\%$, overlying a dense sand layer ($D_R > 90\%$) of the same soil. The model was saturated with methylcellulose pore fluid that had a viscosity that was 40x that of water (40 CST).

Instrumentation within the model included pore pressure transducers and accelerometers, which enabled monitoring the coupled excess porewater pressures and acceleration responses. Piezoceramic bender element pairs were placed at two depths in the model to measure the shear wave velocity. Measurements were performed at 1 g and at 40 g, before and after shaking, for a total of 6 measurements. The processing of bender element time histories is reported by Carey et al. (2021). Horizontal displacement time-histories were measured using highspeed videos of the deforming embankment's cross-section recorded through the transparent side walls of the model container and GEOPIV image analysis software (Carey et al. 2022a).

The ground motion sequence included four shaking motions, all of which included a linear ramp to the maximum acceleration, a hold at the maximum acceleration for a certain number of cycles, and a non-linear decay. All motions had a prototype frequency of 1 Hz but varied in their number of cycles and amplitude of the hold cycles. Further details about the motion are given by Carey et al. (2022a, b). Herein the system response to the motion shown in

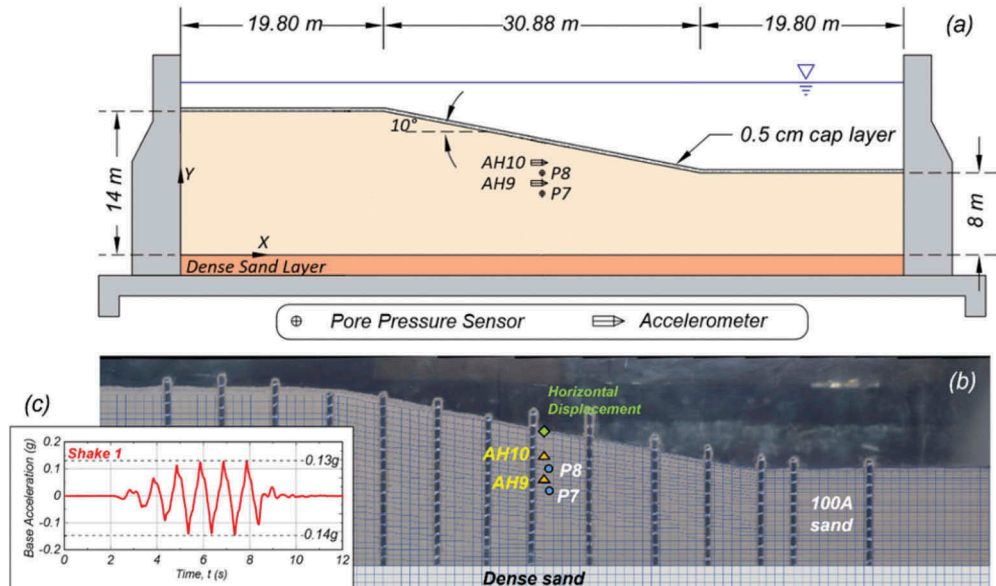


Figure 1. (a) Cross-section of the centrifuge model with accelerometers and porewater pressure sensors (length in prototype scale); (b) FLAC numerical grid used in the simulations overlaid on a photo of the centrifuge model test cross-section; and (c) recorded input motion from the centrifuge experiment used in this study.

Figure 1c with a maximum acceleration of 0.14g is analyzed. For brevity, only the shallowest sensors of the mid-slope array were analyzed (Figure 1a,b).

2.2 Experiment characterization using a CPT

A 10 mm-diameter cone penetrometer was pushed before and after the completion of the ground motion sequence. Cones were pushed into the soil 457 mm at the model scale at a penetration rate of 1 cm/s using a hydraulic actuator (Carey et al. 2022a). Figure 2a presents the CPT profile prior to shaking, measured in the upper bench of the slope.

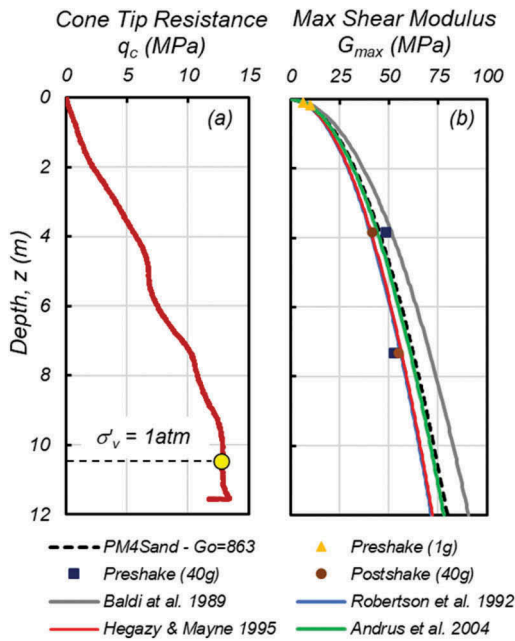


Figure 2. (a) CPT sounding measured prior to the start of the shaking sequence; and (b) comparison of G_{\max} values based on bender elements in the model test with predicted G_{\max} profiles from literature.

Shown in Figure 2a is the pre-shake CPT penetrated to depths that exceeded an overburden stress of 1 atm. Hence, the depth of 10.45 m corresponds to an overburden effective stress of 1 atm and the cone tip resistance, referred to as q_{c1} , was 12.8 MPa. The q_{c1} measurement was sufficiently deep to avoid shallow penetration effects in the model (Kim et al. 2016; Sawyer 2020) and was used to calculate the normalized corrected cone tip resistance, q_{c1N} , as defined by Boulanger & Idriss (2014), which was rounded to 126.0 for the considered case. Since the considered soil has a fines content equal to zero, the 'equivalent clean sand' normalized and corrected cone tip resistance, q_{c1Ncs} , is also 126.0.

3 ESTIMATION OF MODULUS AND CRR

3.1 Estimation of small-strain shear modulus

The shear wave velocity measurements made prior to and following the shaking event were used to calculate the small strain shear modulus, with the values shown in Figure 2b. The small-strain shear modulus at the depth of the atmospheric pressure, $G_{\max,1}$, was calculated according to $G_{\max,1} = pV_s^2$, where p is the soil saturated density of 1,958 kg/m³ at the $D_R = 63\%$.

Several literature relationships expressing the normalized shear wave velocity, V_{S1} , as a function of the cone tip resistance measured in sands were selected and applied using q_{c1N} and are given in Table 1. The laws are expressed by an exponential function:

$$V_{S1} = m q_{c1N}^n \quad (1)$$

where m and n are the coefficients listed in Table 1. The vertical profile of G_{\max} as a function of the mean effective stress, p' , is expressed as:

$$G_{\max} = G_o P_a \left(\frac{p'}{P_a} \right)^{0.5} \quad (2)$$

where P_a is the atmospheric pressure (101.3 kPa) and G_o is the shear modulus coefficient calculated by imposing $G_{\max} = G_{\max,1}$ in Eq. (2) for an effective vertical stress, σ'_v , equal to the atmospheric pressure (Table 1). The mean effective stress, p' is related to the depth, z , as follows:

$$p' = \left(\frac{1+K_0}{2} \right) \sigma'_v = \left(\frac{1+K_0}{2} \right) \gamma' z \quad (3)$$

where K_0 is the coefficient of earth pressure at rest, assumed equal to 0.5, and γ' is the unit weight of the submerged soil. Eq. (2) can be expressed as a function of the depth. As evident in Figure 2b, the bender element-based G_{\max} values were generally consistent with the predicted G_{\max} profiles.

Table 1. Considered V_{S1} – q_{c1N} relationships.

Relationship	m	n	V_{S1}	G_o
	m/s	m/s		
Baldi et al. 1989	110	0.13	206	964
Robertson et al. 1992	60.3	0.23	183	762
Hegazy & Mayne 1995	72.8	0.192	184	769
Andrus et al. 2004	62.6	0.231	191	830

3.2 Estimation of the cyclic resistance ratio

The estimation of the CRR for the 100A sand was obtained through the normalized cone tip resistance q_{c1Ncs} and the CPT-based triggering liquefaction relationship developed by Boulanger & Idriss (2014), as shown in Figure 3. For the q_{c1Ncs} of 126.0, the CRR was equal to 0.186.

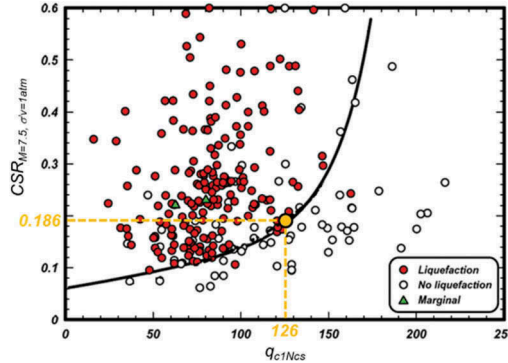


Figure 3. Estimation of CRR from the CPT-based liquefaction triggering curve by Boulanger & Idriss (2014).

4 PM4Sand CALIBRATION

The PM4Sand model calibration based on the experimental CPT data is referred to as “CPT calibration”. The calibration focused on defining the three primary input parameters, D_R , G_o , and h_{po} . The secondary parameters were left to their default values (Boulanger & Ziotopoulou 2017). Specifically, D_R was set to 63%, controlled by the centrifuge test design, and G_o was set to 863, the average of the upper (964) and lower (762) bounds of the G_o relationships in Table 1. The h_{po} parameter of 0.21 was iteratively calibrated via single element undrained cyclic stress-controlled direct simple shear (DSS) simulations until a satisfactory match between the Cyclic Stress Ratio (CSR) and CRR of 0.186 was reached for a triggering criterion of 3% shear strain in 15 cycles.

Figure 4 illustrates CSR versus number of cycles to liquefaction for a 3% single amplitude shear strain triggering criterion for the “CPT calibration”. This curve is generated from a series of single element DSS simulations using the calibrated PM4Sand primary variables, subjected to a range of CSRs. Experimental points as measured through cyclic DSS tests (green points) for two different overburden effective vertical stresses are also plotted for reference. The data for a $\sigma'_{vo} = 50$ kPa were used as the dataset for the laboratory-based calibration (“Lab calibration”) in Chiaradonna et al. (2022).

The cyclic strength at 15 cycles is 0.186 for the “CPT calibration” and 0.133 for “Lab calibration”, implying that the soil resistance to liquefaction as

estimated by the in-situ CPT is 1.4 times higher than that measured by direct simple shear tests.

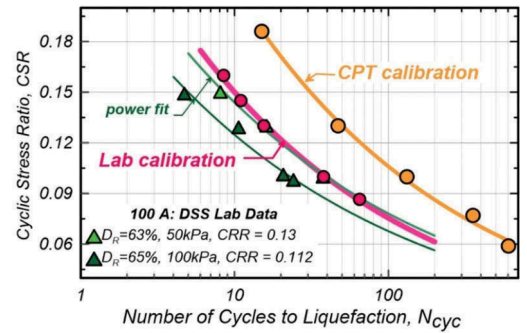


Figure 4. Cyclic resistance curves used in the simulations (CPT calibration) vs calibration based on direct simple shear data (Lab calibration) and experimental data.

5 NUMERICAL SIMULATION RESULTS

The centrifuge test was numerically simulated with the finite difference program FLAC (Itasca, 2016). The geometry of the analysis domain was based on the centrifuge prototype dimensions (Figure 1a). The discretized domain is shown in Figure 1b, with further details available in Chiaradonna et al. (2022).

The predicted and observed time histories of the horizontal displacement at the surface of the mid-slope (Figure 1b) are shown in Figure 5. The experimental trend exhibits a progressive accumulation of displacements, with a final permanent value of 7 cm.

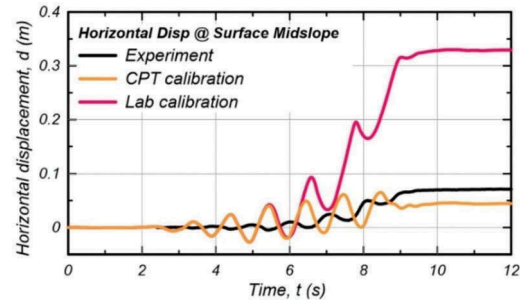


Figure 5. Comparison of horizontal displacement measured at the surface of the embankment slope and numerical simulations from the CPT and Lab calibrations.

The magnitude of the displacement oscillations per cycle is relatively minor, resulting in a clear ratcheting of downslope displacement. The CPT calibration predicted displacements that were practically identical to the experiment with a permanent horizontal displacement was 5 cm. The oscillations in displacements for the CPT calibration are larger compared to the

experiment and predict a dynamic upslope movement. For context, the lab calibration-based simulation predicted significantly higher displacements, with the accumulation primarily occurring during the last two cycles of shaking at full acceleration amplitude and during the decay.

The agreement between the experimentally measured and CPT Calibration simulation of the mid-slope displacement also extended to the global deformation patterns across the centrifuge experiment. This is evident in Figure 6 where contours of horizontal displacement of the experiment are presented. The magnitude and spatial distribution of the displacement field is nearly identical.

While the agreement of the displacement fields is central for performance-based design, examining the pore pressure and acceleration time histories as well as the response spectra at the mid-slope during shaking, is also insightful. Figure 7 presents the pore pressure and acceleration time histories of the upper two locations on the mid-slope. The pore pressure generation time histories for P7 and P8 show different patterns of accumulation, as well as different residual values at the end of shaking. Excess pore pressure ratio, r_u , peaks in P7 are better captured by the “Lab calibration” compared to the “CPT calibration”. The experiment reached an r_u of 1 after several cycles, while the simulation did not. However, at the end of shaking both the experimental and the CPT calibration simulation have a r_u value less than about 0.7, implying that resedimentation and re-establishment of the effective stress profile has been partially taking place.

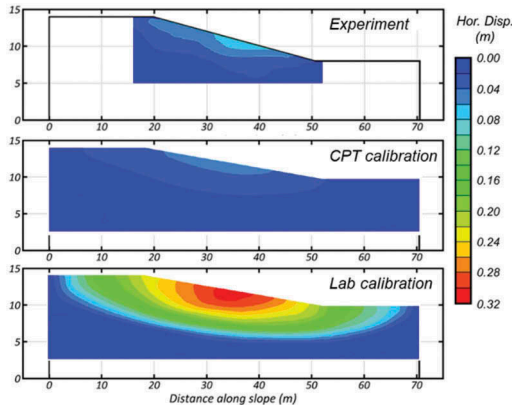


Figure 6. Contour fields of displacement from the shake measured in the centrifuge experiment, and the numerically predicted contours using the CPT and Lab PM4Sand calibrations.

The acceleration time histories between the measured experimental response and the CPT calibration simulation are nearly identical for the lower AH9 accelerometer, time history, and in the first part of the AH10 time history. However, later in the AH10 time

history the predicted accelerations in the simulation are lower. These trends are also evident in the clear agreement in the spectral acceleration plots for AH9, with show consistency across all periods. For AH10 the higher spectral acceleration at the predominant period of 1 Hz is evident. For periods less than 0.7 s, spectral accelerations are better captured better by the “Lab calibration” due to the dilation spikes in the time histories of acceleration; however, these high frequencies have a minor contribution to the overall movement of the embankment.

The agreement in deformation, acceleration, acceleration response spectra, and excess porewater pressure trends stand in clear contrast to the trends for the “Lab Calibration” simulation. As evident in Figures 6 and 7 the displacements that accumulate near the end and after shaking are significantly larger at the mid-slope surface and throughout much of the model. The primary reason for these differences is attributed both (1) to the lower cyclic resistance ratio (CRR) of the laboratory data which contributes to an early onset of liquefaction and its associated deformations, and (2) the continuing deformation after the end of shaking due a high excess pore pressure.

6 DISCUSSION

The numerical simulation presented in this paper demonstrates the utility and value of CPT measurements in centrifuge experiments. Simulations based on a CPT-based calibration of the PM4Sand constitutive model provided a very satisfactory match to the observed system level responses. Past parametric investigations by Chiaraonetta et al. (2022) had shown that a CRR higher than the one obtained from DSS tests would likely justify the observed responses.

However, that study was inconclusive as to whether the higher in-situ CRR was an artifact of arching or sloping ground conditions or that in general the DSS data in this case had misrepresented the in-situ centrifuge conditions. The present study demonstrated that the CPT measurements provided a significantly improved characterization of the cyclic resistance of the centrifuge model and thus a more successful validation of the response, particularly with respect to displacements.

Future work will investigate the (i) influence of other contributing factors such as 3D effects and arching, (ii) effect of sloping ground conditions on cyclic strength, and (iii) reasons between the discrepancy of the DSS-based CRR and the CPT-based CRR.

7 CONCLUDING REMARKS

This paper addressed the calibration of a critical state compatible, stress ratio-based, bounding surface plasticity constitutive model aiming at

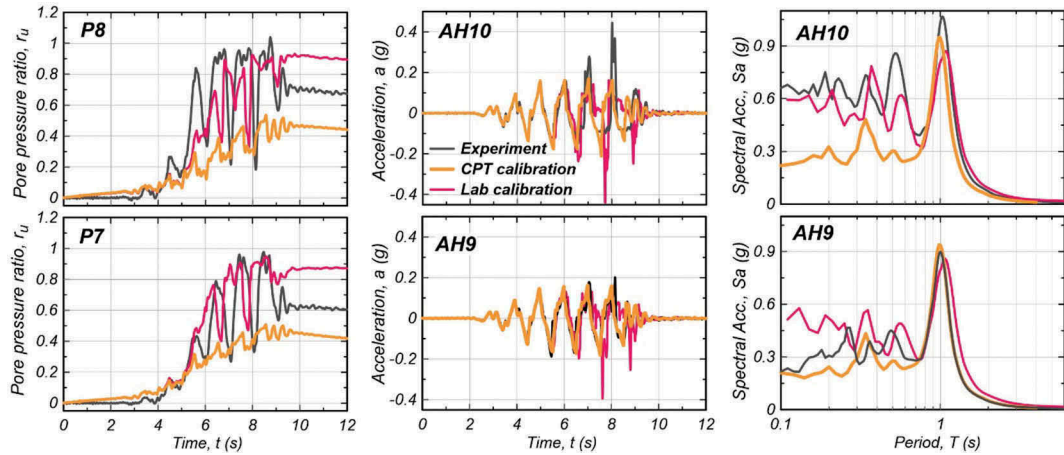


Figure 7. Comparison of the measured experimental and numerically simulated responses for ‘CPT Calibration’ vs. ‘Lab Calibration’. Results are for the select sensors (Figure 1) in terms of porewater pressure ratio, acceleration time histories, and response spectra (5% damping).

numerically simulating the dynamic behavior of a poorly-graded sand slope. While deficiencies in the horizontal displacement prediction were highlighted by a calibration obtained from cyclic laboratory tests (Chiaradonna et al. 2022), the use of CPT data as a calibration basis produced a better prediction of both displacements and accelerations. The reliability of the simulation can be ascribed mainly to two principal reasons: (i) the cyclic strength of the soils is directly estimated by combining the measured cone tip resistance of the soil tested in centrifuge with the CPT-based triggering liquefaction chart, and (ii) the small-strain shear modulus is well reproduced by the applied literature relationships for clean sands. This study strengthens the importance of in-flight CPT measurements in centrifuge tests and represents a step forward in the calibration of advanced constitutive models using measurements from in-situ CPT tests. Further applications to available centrifuge tests with different relative densities and gradation of soils will be performed to generalize the obtained results.

ACKNOWLEDGEMENTS

The National Science Foundation (NSF) provided funding for this work (Grant No. CMMI-1916152) and for the Natural Hazards Engineering Research Infrastructure (NHERI) centrifuge facility at UC Davis (Grant No. CMMI-1520581). Any opinions, findings, and conclusions, or recommendations expressed in this material are those of the author(s) and do not necessarily reflect those of the NSF. The lead author was supported by the U.S. Fulbright Scholar Program.

REFERENCES

Andrus, R.D., Piratheepan, P., Ellis, B.S., Zhang, J. & Juang, C.H. 2004. Comparing liquefaction evaluation methods using penetration- V_S relationships. *Soil Dyn. Earthq. Eng.* 24: 713–721.

Baldi, G., Bellotti, R., Ghionna, V., Jamiolkowski, M. & Lo Presti, D.C.F. 1989. Modulus of sands from CPTs and DMTs. *Proc. 12th Int. Conf. on Soil Mech. and Found. Eng.*, Rio de Janeiro, 13–18 August 1989. Vol. 1: 165–170. Rotterdam: Balkema.

Boulanger, R.W. & Idriss, I.M. 2014. *CPT and SPT liquefaction triggering procedures*. Report No UCD/GCM-14/01, University of California at Davis, California, USA.

Boulanger, R.W. & Ziotopoulou, K. 2017. *PM4Sand (Version 3.1): A sand plasticity model for earthquake engineering applications*. Technical Report No. UCD/CGM-17/01, Center for Geotechnical Modeling, University of California, Davis.

Carey, T.J., Chiaradonna, A., Love, N., DeJong, J.T., Ziotopoulou, K., Martinez, A. 2021. *Effect of soil gradation on the response of a submerged slope when subjected to shaking –centrifuge data report for TJC01*. Report No. UCD/CGM-21/03, University of California at Davis, California, USA.

Carey, T.J., Chiaradonna, A., Love, N., Wilson, D.W., Ziotopoulou, K., Martinez, A. & DeJong, J.T. 2022a. Effect of soil gradation on embankment response during liquefaction: a centrifuge testing program. *Soil Dyn. Earthq. Eng.* (Under review).

Carey, T.J., DeJong, J.T., Ziotopoulou, K., Martinez, A. & Chiaradonna, A. 2022b. The effects of gradation on the dynamic response of sloping ground. *Proc. 20th Intern. Conf. on Soil Mech. & Geotech. Eng.*, Sydney, 1–5 May 2022 (Accepted).

Carey, T.J., Gavras, A. & Kutter, B.L. 2020. Comparison of LEAP-UCD-2017 CPT Results. In *Model Tests and Numerical Simulations of Liquefaction and Lateral Spreading*: 117–129. Cham: Springer.

Chiara donna, A., Ziotopoulou, K., Carey, T.J., DeJong, J.T. & Boulanger, R.W. 2022. Dynamic Behavior of Uniform Clean Sands: Evaluation of Predictive Capabilities in the Element- and the System-Level Scale. *GeoCongress 2022, Charlotte, 20–23 March 2022* (Accepted paper).

Darby, K.M., Boulanger, R.W., DeJong, J.T. & Bronner, J.D. 2019. Progressive Changes in Liquefaction and Cone Penetration Resistance across Multiple Shaking Events in Centrifuge Tests. *J. Geotech. Geoenviron. Eng.*, ASCE 145(3).

Hegazy, Y.A. & Mayne, P.W. 1995. Statistical correlations between VS and cone penetration data for different soil types. *Proc. 1st International Symposium on Cone Penetration Testing, CPT '95, Linkoping, 4-5 October 1995*, 2: 173–178.

Humire, F., Ziotopoulou, K. & DeJong, J.T. 2022. Evaluating shear strain accumulation of sands exhibiting cyclic mobility behavior. *Proc. 20th Intern. Conf. on Soil Mech. and Geotech. Eng., Sydney, 1–5 May 2022* (Accepted paper).

Itasca 2020. FLAC – Fast Lagrangian Analysis of Continua, Version 8.1. Minneapolis, MN: Itasca Consulting Group.

Kamai, R., & Boulanger, R.W. (2011). Characterizing localization processes during liquefaction using inverse analyses of instrumentation arrays. *Meso-Scale Shear Physics in Earthquake and Landslide Mechanics*, 219–238.

Khosravi, M., Boulanger, R.W., DeJong, J.T., Khosravi, A., Hajialilue-Bonab, M. & Wilson, D.W. 2018. Centrifuge modeling of cone penetration testing in layered soil. In *Geotechnical Special Publication 290*, S. J. Brandenberg and M. T. Manzari (eds.); *Proc. Geotechnical Earthquake Engineering and Soil Dynamics V, Austin, 10–13 June 2018*.

Kim, J.H., Choo, Y.W., Kim, D.J. & Kim, D.S. 2016. Miniature cone tip resistance on sand in a centrifuge. *J. Geotech. Geoenviron. Eng.*, ASCE 142 (3).

Moug, D.M., Price A.B., Bastidas, A.M.P., Darby, K.M., Boulanger, R.W. & DeJong, J.T. 2019. Mechanistic Development of CPT-Based Cyclic Strength Correlations for Clean Sand. *J. Geotech. Geoenviron. Eng.*, ASCE 145(10).

Robertson, P.K., Woeller, D.J. & Finn, W.D.L. 1992. Seismic CPT for evaluating liquefaction potential. *Canadian Geotechnical Journal* 29: 686–695.

Sawyer, B.D. 2020. *Cone penetration testing of coarse-grained soils in the centrifuge to examine the effects of soil gradation and centrifuge scaling*. Master's Thesis. UC Davis.

Sturm, A.P. 2019. *On the Liquefaction Potential of Granular Soils: Characterization, Triggering and Performance*. PhD Dissertation. UC Davis.